Switch Status Identification in Distribution Networks using Harmonic Synchrophasor Measurements

Lei Chen, *Student Member, IEEE*, Mohammad Farajollahi, *Student Member, IEEE*, Mahdi Ghamkhari, *Member, IEEE*, Wei Zhao, Songling Huang, *Senior Member, IEEE*, and Hamed Mohsenian-Rad, *Fellow, IEEE*

***Abstract*—witch status identification (SSI)witch status identification (SSI)S in distribution networks is a challenging task due to the limited measurement resources and therefore the inevitable need is to use pseudo-measurements that are often inaccurate. To address this issue, a new method is proposed in this paper to integrate *harmonic synchrophasors* into the SSI problem in order to enhance SSI accuracy in distribution networks. In this method, switch status identification is done *jointly* based on both fundamental synchrophasor measurements and harmonic synchrophasor measurements. This is done by formulating and then solving a mixed-integer linear programming (MILP) problem. Furthermore, an analysis is provided to capture the number of and the location of harmonic sources and sensors that are needed to ensure full observability. The benefits of the proposed SSI scheme are compared against those of the traditional scheme that utilizes only the fundamental measurements. The efficiency of the proposed method is demonstrated through numerical simulations on IEEE 33-Bus and 123-Bus test systems. The results show the advantage of using harmonic information in SSI over the traditional SSI schemes using sole fundamental measurements.**

***Index Terms*—Harmonic synchrophasor, phasor measurement units, distribution networks (DNs), switch status identification, DN topology.**

I. Introduction

A. Background and Motivations

Knowing the topology of distribution network (DN) is crucial for power distribution system operation, and comes with various applications such as event source location [1], state estimation [2], and line impedance estimation [3]. The topology is known if one identifies the status of the switches in all line segments. If the changes in the status of the switches are not identified, the accurate topology of the power system will be lost and large errors will occur in the mentioned applications that rely on knowing the topology of the DN.

The problem of switch status identification (SSI) is of importance in both distribution and transmission networks. In transmission networks, there are often either sensors that directly identify the status of switches or there are sufficient measurements to achieve full observability to estimate the status of switches. However, conducting SSI is more challenging when it comes to distribution systems. In particular, due to the lack of sufficient measurements in DNs, there is often a need to highly rely on pseudo-measurements in order to solve the SSI problem. However, given the inherent inaccuracy in pseudo-measurements, they may cause incorrect switch status identification. This issue motivates us to propose a new SSI scheme to reduce SSI errors caused by the lack of enough measurements.

Using other sources of information available at DNs for the SSI task may be a solution to such an issue. As an important one, harmonic currents are present in DNs as a result of utilizations of non-linear devices such as power electronic inverters. Also, a new generation of phasor measurement units have been developed recently that can report not only the fundamental synchrophasors but also the harmonic current synchrophasors with high accuracy [4]–[7]. These types of PMUs are already installed in multiple pilot utilities, such as the ones in Japan [8].

The use of harmonic measurements for SSI task is motivated by two features of harmonic currents in DNs, which make them quite different from fundamental currents and thus useful for SSI: 1) the sources of harmonic currents are located in the load side in contrast to the source of fundamental current that is in the substation side; and 2) only a few types of loads can generate considerable amounts of harmonic currents. These two features are useful to identify the status of the branches falling on a harmonic current path to help correctly estimate the switch status misidentified in the traditional SSI scheme that uses merely fundamental current measurements. The advantages of leveraging the harmonic information in SSI problem is discussed in Sections VI-A and VI-C.

B. Related Works

In literature, several works attempted to identify the DN switch status by using the knowledge of the set of all possible topologies [9]–[11]. All of these works assume that the voltage of each node in the DN can be measured by a voltage sensor or a smart meter. However, this may not be realistic in practice because in some DNs only the voltage measurements of some nodes, not all nodes, are available [11].

Lei Chen, Wei Zhao, and Songling Huang are with the State Key Lab. of Power System, Department of Electrical Engineering, Tsinghua University, Beijing, 100084, China. The method in this paper was developed when Lei Chen was a visiting PhD student at the University of California, Riverside, USA.

Mohammad Farajollahi and Hamed Mohsenian-Rad are with the Department of Electrical and Computer Engineering, University of California, Riverside, CA, USA.

Mahdi Ghamkhari is with the Electrical and Computer Engineering Department of University of Louisiana at Lafayette, Lafayette, LA, USA.

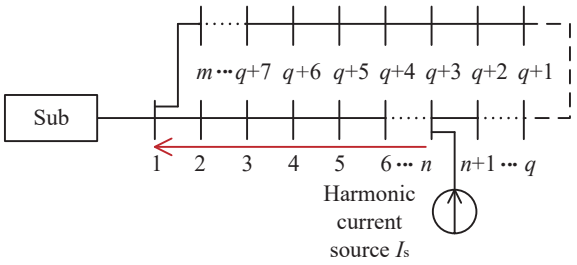

Fig. 1. An illustration of harmonic current flow in radial DNs. The branch (q, q+1) is normally open, and other branches are normally closed. The harmonic current path is shown by a red arrow line, i.e., from node n to the substation.

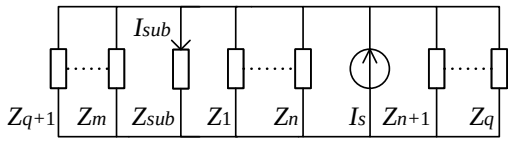

Fig. 2. Equivalent impedance network of the DN in Fig. 1. Z_{sub} is the equivalent impedance of the substation. Z_n is the impedance of the load at node n.

There also exist several data-driven methods which can estimate the DN switch status without knowing the set of all possible topologies [12]–[14]. These methods generally use data samples from several hours to several days for training the SSI model, and thus assume that the DN switch status has undergone no change during the sampling collection. However, such assumption is not valid considering that the DN switch status may change frequently due to some tasks like optimal reconfiguration. Several studies [15], [16] proposed other data-driven methods that are specifically designed to resolve the issue with such assumption. However, all these data-driven methods may not be applicable in a DN due to their need for large number of measurements.

To address the issue with the deficiency of measurements in distribution system, several SSI methods has been introduced based on the pseudo-measurements [17]–[20]. They generally use fundamental measurements to formulate a linear programming problem. Among them, [17] is the closest work to the proposed SSI scheme. PMU installation requirements for solving the MILP problem are also analyzed in [17]. The method proposed in [17] does not show a good performance once the pseudo-measurements are highly erroneous. In this regard, we aim to use the harmonic measurements as another source of information to compensate the deficiency associated with the pseudo-measurements. This paper combines both fundamental and harmonic synchrophasor measurements to formulate an SSI problem that comes with an improved accuracy even in the presence of large pseudo-measurement errors.

C. Summary of Contributions

The main contributions of the paper are as follows:

- To the best of our knowledge, this is the first paper that proposes using harmonic synchrophasor measurements to identify the switch status of distribution system.
- The proposed method works by integrating a harmonic SSI problem formulation with a fundamental SSI problem formulation through introducing several conjunction equations to leverage both fundamental and harmonic measurements to identify the DN switch status.
- One outstanding merit of the proposed SSI scheme is that it does *not* require placement of additional PMUs in DNs but rather utilizes *additional information*, i.e. harmonic currents, available from the existing PMUs.
- Through computer simulations, it is shown that the accuracy of the proposed SSI scheme is at least 10% more than that of the traditional scheme which uses only measurements of the fundamental currents.
- An analysis is provided that specifies the number of and the location of the harmonic resources and PMUs that are required to ensure full observability of the DN.

This paper gives focus to the study of SSI in radial networks, as DNs are mostly with radial topology [20].

II. Harmonic Currents in Radial Networks

When it comes to the steady-state analysis of harmonics in DN, nonlinear loads can be modeled by a harmonic current source and a shunt admittance [21] (more discussions about harmonic source characteristics on harmonic source modeling can be found in [22]). We assume that there exist no harmonic resonance in the DN under study. This assumption is justified by the fact that, harmonic resonance may occur only when the resonant frequency coincides with a harmonic frequency, which may happen only rarely. Besides, there exist mature techniques to damp harmonic resonance [23]. Under the said assumption, the load shunt impedance is much larger than the DN lines impedance and equivalent harmonic impedance of the substation, see [21] for more details. As a result, almost all of the harmonic source current is injected into the substation and the harmonic current injected to the load can be neglected.

Consider the power distribution system in Fig. 1, whose topology depends on the status of the segmental switches. Its corresponding equivalent impedance network is as shown in Fig. 2. The harmonic current injection to the substation can be calculated as follows:

$$I_{sub} = \frac{\frac{1}{Z_{sub}}}{\sum_{n=1}^{m} \frac{1}{Z_n} + \frac{1}{Z_{sub}}} I_s = \frac{1}{\sum_{n=1}^{m} \frac{Z_{sub}}{Z_n} + 1} I_s \approx I_s, \quad (1)$$

From (1), we see that almost all of the harmonic currents coming from node n are being injected into the substation. Accordingly, for every harmonic source we can define the *harmonic current path* as the path of harmonic current which is flowing from the node with the harmonic source to the substation. For example, the red line in Fig. 1 is a harmonic current path corresponding to the harmonic source at node n. In a radial DN, there is only one harmonic current path for each harmonic source, but a branch of the DN can correspond to several harmonic current paths. Thus, the harmonic currents of the branches falling on at least one harmonic current path can be the *combination* of several harmonic sources with the same harmonic frequency. For instance, if there are two harmonic sources with currents of 1 A and 2 A (which are

both at a same frequency), then the possible combinations of the harmonic sources, i.e. the possible harmonic currents of the branches falling on at least one harmonic current path, could be 1 A, 2 A, and 3 A.

To identify the status of a branch as closed, it suffices to show that the branch falls on at least one harmonic current path. Nevertheless, the status of a branch cannot be identified as either closed or open if the branch carries no harmonic current. Rather, to identify the status of a branch as open one needs to detect a loop, in which only the single branch of interest does not fall on any harmonic current path. In that case, the switch on the branch of interest must be open.

The above methodology in identifying open switches is based on the fact that, in a DN with radial topology, at least one branch must be open in every loop of branches. For example, in the power system of Fig. 1 which includes only one loop the branch $(q, q+1)$ must be open if there is a harmonic current on every branch except on the branch $(q, q+1)$.

In summary, carrying no harmonic current is a necessary but not sufficient condition for a branch to be identified as open. The status of a switch with no harmonic current can be identified as open only by detecting a loop with the said conditions.

Please note that although the impedances of the distribution lines are different in different harmonic frequencies, they are always much smaller than the load impedances. This factor corroborates the conclusion in (1). In practice, different harmonic components may exist in a DN. The domination of one harmonic component over the other components depends on the structure of DN and the harmonic source magnitudes [22]. For example, in a delta system there could be no 3^{rd} harmonic current flowing through distribution lines while the flow of 7^{th} harmonic currents can exist. For such a system, the 3^{rd} harmonic currents cannot be selected for the SSI while the 7^{th} harmonic source currents can be. In general, the dominant harmonic current in the DN should be selected for the TI.

If multiple harmonic components, not just the component with the largest currents, are taken into consideration, the redundancy of the SSI is improved and the SSI results will be guaranteed. However, this paper just uses one harmonic component, and proposing an SSI scheme using multiple harmonic components will be included in the future work.

III. Switch Status Identification in a Nonlinear Optimization Framework

In this section, an SSI scheme is proposed that utilizes both the fundamental and harmonic current measurements in DNs. The proposed SSI scheme is formulated as a nonlinear optimization problem.

A. Partial Switch Status Identification based on Harmonic Currents

In general, dedicated sensors are installed in DNs to monitor the harmonic current injections of large nonlinear loads, such as the power quality sensors [24], [25]. On this account, we assume that the harmonic source current measurements of these large nonlinear loads are available for SSI. For small nonlinear loads, there may not exist devices to measure harmonic source currents. In this paper, the harmonic currents of these small sources are assumed as 0. Let I_i^h denote the current of the h^{th} harmonic component associated with the harmonic source located at node i. According to the Kirchhoff's Current Law (KCL) we have:

$$\sum_{j\in\mathcal{N}_i} I^h_{(i,j)} = I^h_i \quad \forall i \in \mathcal{K}, \tag{2}$$

where $I^h_{(i,j)}$ is the h^{th} harmonic current on branch (i,j); $\mathcal{K}$ is the set of nodes containing harmonic sources; and $\mathcal{N}_k$ is the set of nodes connected to the node k. For the nodes with no harmonic sources and the nodes with a small harmonic sources without monitoring devices, we have:

$$\sum_{j\in\mathcal{N}_i} I^h_{(i,j)} = 0 \quad \forall i \in \mathcal{N}, i \notin \mathcal{K}, \tag{3}$$

where $\mathcal{N}$ is the set of all nodes in the DN.

As was discussed in Section II, detecting the paths of harmonic currents is vital in identifying the status of the switches in the DN. To this end, one needs to examine whether or not a branch carries a harmonic current. This can be done by looking into the numerical value of $I^h_{(i,j)}$. More precisely, if $I^h_{(i,j)}$ is larger than the magnitude of the smallest-magnitude combination of all existing harmonic sources in the DN, i.e. the parameter z, then the branch must be on a harmonic current path. To simplify the analysis, we make two adjustments. First, instead of assessing the magnitude of harmonic current $I^h_{(i,j)}$ we choose to assess the absolute values of the real and imaginary parts of the harmonic current $I^h_{(i,j)}$. Second, instead of using the parameter z in the comparisons, we use a threshold parameter c that is less than the parameter z. This is because the actual harmonic current flowing through a harmonic current path may be smaller than z due to the error in PMU measurements. In order to ensure that the harmonic current paths can be detected correctly, a threshold parameter c is used that is less than the parameter z. To this end, we first obtain the absolute values of the real and imaginary parts of the harmonic current $I^h_{(i,j)}$ as follows:

$$\text{Re}\{I^h_{(i,j)}\} = 2q^{h,re}_{(i,j)} X^{h,re}_{(i,j)} - X^{h,re}_{(i,j)} \quad \forall (i,j) \in \mathcal{B} \tag{4}$$

$$\text{Im}\{I^h_{(i,j)}\} = 2q^{h,im}_{(i,j)} X^{h,im}_{(i,j)} - X^{h,im}_{(i,j)} \quad \forall (i,j) \in \mathcal{B} \tag{5}$$

$$X^{h,re}_{(i,j)} \geq 0;\ X^{h,im}_{(i,j)} \geq 0 \qquad \forall (i,j) \in \mathcal{B}, \tag{6}$$

where $\mathcal{B}$ is the set of all branches; $q^{h,re}_{(i,j)}$ and $q^{h,im}_{(i,j)}$ are binary variables; $X^{h,re}_{(i,j)}$ and $X^{h,im}_{(i,j)}$ are non-negative variables; and the superscripts ^{re} and ^{im} indicate real and imaginary parts, respectively. If the real or imaginary part of $I^h_{(i,j)}$ is positive, then $q^{h,re}_{(i,j)}$ or $q^{h,im}_{(i,j)}$ must be 1 and $X^{h,re}_{(i,j)}$ or $X^{h,im}_{(i,j)}$ must be equal to the real or imaginary part of $I^h_{(i,j)}$, respectively. If the real or imaginary part of $I^h_{(i,j)}$ is negative, then $q^{h,re}_{(i,j)}$ or $q^{h,im}_{(i,j)}$ must be 0 and $X^{h,re}_{(i,j)}$ or $X^{h,im}_{(i,j)}$ must be equal to the absolute value of the real or imaginary part of $I^h_{(i,j)}$, respectively. All in all, we see that the absolute values of the real and imaginary parts of $I^h_{(i,j)}$ are $X^{h,re}_{(i,j)}$ and $X^{h,im}_{(i,j)}$, respectively.

Next, we compare the summation of the variables $X^{h,re}_{(i,j)}$ and $X^{h,im}_{(i,j)}$ against the threshold c to see whether or not the branch (i,j) falls on any harmonic current path. The harmonic current flowing through a branch may be the combination of several harmonic sources at different nodes of the DN. If the branch (i,j) is not on any harmonic current path, then we must have $X^{h,re}_{(i,j)} + X^{h,im}_{(i,j)} \leq c$. In contrast, if the branch (i,j) is on a harmonic current path, we must have $X^{h,re}_{(i,j)} + X^{h,im}_{(i,j)} \geq c$. The comparison between $X^{h,re}_{(i,j)} + X^{h,im}_{(i,j)}$ and the threshold parameter c can be mathematically formulated by the following constraint:

$$(1 - b^h_{(i,j)})[(X^{h,re}_{(i,j)} + X^{h,im}_{(i,j)}) - c] + b^h_{(i,j)}[c - (X^{h,re}_{(i,j)} + X^{h,im}_{(i,j)})] \leq 0 \quad \forall (i,j) \in \mathcal{B}, \quad (7)$$

where $b^h_{(i,j)}$ is a binary variable. From (7), the numerical values of 0 and 1 for the binary variable $b^h_{(i,j)}$ translate to the inequalities of $X^{h,re}_{(i,j)} + X^{h,im}_{(i,j)} \leq c$ and $X^{h,re}_{(i,j)} + X^{h,im}_{(i,j)} \geq c$, respectively. Consequently, numerical values of $b^h_{(i,j)} = 0$ and $b^h_{(i,j)} = 1$ correspond to the branch (i,j) not being on any harmonic current path and being on at least one harmonic current path, respectively.

It is worth mentioning that although two binary variables $q^{h,re}_{(i,j)}$ and $q^{h,im}_{(i,j)}$ are used to detect whether the harmonic branch current is 0 or not, the usage of binary variable $b^h_{(i,j)}$ is inevitable. In the ideal condition, i.e., all harmonic source currents are injected to the DN, the harmonic currents of the branches not falling on any harmonic current paths will be definitely 0. However, in reality not all harmonic source currents are injected to the DN, and there must be harmonic current injections into the other nodes that do not have harmonic sources. In such a case, the harmonic currents of the branches not falling on any harmonic current path will not be 0. Hence, the binary variable $b^h_{(i,j)}$ is used to distinguish whether a branch is falling on a harmonic current path or not.

From the discussion in section II, we know that a numerical value of 1 for the binary variable $b^h_{(i,j)}$ testifies the in-service status of the branch (i,j), but a numerical of 0 for the binary variable $b^h_{(i,j)}$ doesn't indicate the in-service or out-of-service status for the branch. As a result, additional information is needed to determine the status of all the branches. This can be done by looking into the fundamental currents measurements.

B. Switch Status Identification using Fundamental Currents

According to the KCL we have:

$$\sum_{j \in N_i} I_{(i,j)} = I_i \quad \forall i \in \mathcal{N}, \quad (8)$$

where $I_{(i,j)}$ is the fundamental current on branch (i,j); and I_i is the fundamental current injection into the node i, which can be obtained from the pseudo-measurements, i.e., the measurements estimated from the seasonal load curves. The status of the branch (i,j) can be modeled by the following constraint:

$$-M s_{(i,j)} \leq I_{(i,j)} \leq M s_{(i,j)} \quad \forall (i,j) \in \mathcal{B}. \quad (9)$$

where M is a large number selected arbitrarily and $s_{(i,j)}$ is a binary variable. A numerical value of 1 for the binary variable $s_{(i,j)}$ corresponds to the in-service status for the branch (i,j) and requires the fundamental current $I_{(i,j)}$ to be within the interval of $[-M, M]$. In contrast, a numerical value of 0 for the binary variable $s_{(i,j)}$ corresponds to the out-of-service status for the branch (i,j) and requires the fundamental current $I_{(i,j)}$ to be 0.

C. Switch Status Identification based on Fundamental and Harmonic Currents

So far, we have explained how measurements of fundamental and harmonic currents can be used to derive the status of the switches. However, to integrate both fundamental and harmonic into on SSI problem, we need to derive the relationships between the binary variables $b^h_{(i,j)}$ and $s_{(i,j)}$. $b^h_{(i,j)} = 1$ indicates that the switch is closed which enforces $s_{(i,j)} = 1$. Also, $s_{(i,j)} = 0$ indicates that the switch is open which enforces $b^h_{(i,j)} = 0$. Finally, when $b^h_{(i,j)}$ is 0 the corresponding switch can be open or closed and accordingly $s_{(i,j)}$ can be 0 or 1. These relationships between the binary variables $b^h_{(i,j)}$ and $s_{(i,j)}$ can be modeled by the following constraint:

$$b^h_{(i,j)} \leq s_{(i,j)} \quad \forall (i,j) \in \mathcal{B}. \quad (10)$$

Besides the relationships between the fundamental and harmonic switch binary variables, there is a further relationship between the fundamental switch binary variables which should be taken into account. The following equation establishes another relationship between the binary variables $s_{(i,j)}$, using the fact that in every loop of a radial network at least one switch must be open:

$$\sum_{(i,j) \in \mathcal{L}} s_{(i,j)} \leq N_l - 1 \quad \forall \mathcal{L} \in \mathcal{P}, \quad (11)$$

where $\mathcal{L}$ is the set of all branches in an arbitrary loop of the DN; $\mathcal{P}$ is the set of all the possible loops in the DN, which can be formed using the algorithm provided in [26]; and N_l is the number of branches in the loop $\mathcal{L}$. In order to find the set of possible loops $\mathcal{P}$, the planning model of the DN should be known. In finding the set of possible loops $\mathcal{P}$, all the lines are assumed to be closed [26]. For (11), we notice that if in a loop $\mathcal{L}$ of the radial network $N_l - 1$ switches turn out to be closed from the harmonic currents analysis, the binary variables $s_{(i,j)}$ for all these $N_l - 1$ switches are enforced to be 1. Then the binary variable $s_{(i,j)}$ for the last remaining switch of the loop $\mathcal{L}$ must be 0, which requires the last switch to be open. Therefore, (11) addresses the said condition at the end of section II to identify the status of the switch with no harmonic current.

Finally, there is another relationship between all the binary variables $s_{(i,j)}$ which ensures the radial configuration of the DN [19]:

$$\sum_{(i,j) \in \mathcal{B}} s_{(i,j)} = N - 1, \quad (12)$$

where N is the total number of nodes in the DN.

Let $I^{h,m}_{(i,j)}$ and $I^{m}_{(i,j)}$ denote the measurements of harmonic and fundamental currents, respectively, collected by PMUs. The following optimization problem minimizes the error in the estimation of harmonic and fundamental currents in the DN [17]:

$$\begin{aligned} \textbf{Min} \quad & \sum_{(i,j)\in\mathcal{M}} \frac{|I^{h}_{(i,j)} - I^{h,m}_{(i,j)}|}{|I^{h,m}_{(i,j)}|} + \frac{|I_{(i,j)} - I^{m}_{(i,j)}|}{|I^{m}_{(i,j)}|} \\ \textbf{s.t.} \quad & \text{Eqs } (2) \sim (12), \end{aligned} \tag{13}$$

where $\mathcal{M}$ is the set of all branches equipped with PMUs; $I^{h,m}_{(i,j)}$ denotes the harmonic current phasor which can be obtained by any synchronized power quality sensors. It should be noted that, in problem (13), we minimize the *normalized* values of the errors. If the accuracy is not the same for the fundamental and harmonic measurements, then we may include some coefficients in the objective function in (13) to further adjust normalization. In summary, the proposed SSI scheme in (13) uses the *estimated* harmonic and fundamental currents of each branch to identify the switch status. Although some branches may carry zero harmonic currents, the corresponding switch status is identified by using fundamental information. In nutshell, if the harmonic and fundamental currents associated with a branch are both estimated as zero, this branch is out-of-service, otherwise it is in-service.

It is worth mentioning that that the proposed SSI scheme in (13) is just working for the radial distribution systems, not meshed systems. Please also note that, the proposed SSI scheme needs the following inputs: 1) fundamental currents and harmonic currents flowing through some branches, which are measured by the PMUs; 2) harmonic source currents from the large nonlinear loads, which are measured by power quality devices or harmonic monitoring devices; 3)fundamental pseudo-current injections of all the nodes, which are obtained from the seasonal load curves [20].

IV. Switch Status Identification in a Linear Optimization Framework

The proposed SSI scheme formulated in (13) is an MINLP problem, while no algorithm is yet developed to guarantee to solve this problem. Thus, in this section we take several steps to reformulate the problem in (13) to a solvable MILP format.

A. Tackling the Non-Linearity in the Constraints

In problem (13), the constraints (4), (5), and (7) include non-linear terms. All the non-linear terms are formed by the product of a binary variable and a continuous variable. The non-linear constraint (4) in problem (13) can be replaced with the following linear constraints:

$$\mathrm{Re}\{I^{h}_{(i,j)}\} = 2W^{h,re}_{(i,j)} - X^{h,re}_{(i,j)} \quad \forall (i,j) \in \mathcal{B} \tag{14}$$

$$-Mq^{h,re}_{(i,j)} \le W^{h,re}_{(i,j)} \le Mq^{h,re}_{(i,j)} \quad \forall (i,j) \in \mathcal{B} \tag{15}$$

$$-M(1-q^{h,re}_{(i,j)}) \le W^{h,re}_{(i,j)} - X^{h,re}_{(i,j)} \le M(1-q^{h,re}_{(i,j)}) \quad \forall (i,j) \in \mathcal{B}, \tag{16}$$

where $W^{h,re}_{(i,j)}$ is a new continuous optimization variable. A similar approach can be taken to replace the non-linear constraints (5) and (7) with linear ones. As a result, the constraint (5) can be replaced by the following constraints:

$$\mathrm{Im}\{I^{h}_{(i,j)}\} = 2W^{h,im}_{(i,j)} - X^{h,im}_{(i,j)} \quad \forall (i,j) \in \mathcal{B} \tag{17}$$

$$-Mq^{h,im}_{(i,j)} \le W^{h,im}_{(i,j)} \le Mq^{h,im}_{(i,j)} \quad \forall (i,j) \in \mathcal{B} \tag{18}$$

$$-M(1-q^{h,im}_{(i,j)}) \le W^{h,im}_{(i,j)} - X^{h,im}_{(i,j)} \le M(1-q^{h,im}_{(i,j)}) \quad \forall (i,j) \in \mathcal{B}. \tag{19}$$

where $W^{h,im}_{(i,j)}$ is a new continuous optimization variable to replace the nonlinear term $q^{h,im}_{(i,j)} X^{h,im}_{(i,j)}$ in (5). Similarly, the constraint (7) can be replaced by the following constraints:

$$2cb^{h}_{(i,j)} - 2X^{h}_{(i,j)} + X^{h,re}_{(i,j)} + X^{h,im}_{(i,j)} - c \le 0 \quad \forall (i,j) \in \mathcal{B} \tag{20}$$

$$-Mb^{h}_{(i,j)} \le X^{h}_{(i,j)} \le Mb^{h}_{(i,j)} \quad \forall (i,j) \in \mathcal{B} \tag{21}$$

$$-M(1-b^{h}_{(i,j)}) \le X^{h}_{(i,j)} - (X^{h,re}_{(i,j)} + X^{h,im}_{(i,j)}) \le M(1-b^{h}_{(i,j)}) \quad \forall (i,j) \in \mathcal{B}. \tag{22}$$

where $X^{h}_{(i,j)}$ is a new continuous optimization variable to replace the nonlinear term $b^{h}_{(i,j)}(X^{h,re}_{(i,j)} + X^{h,im}_{(i,j)})$ in (7).

B. Tackling the Non-Linearity in the Objective Function

The non-linearity of the objective function in problem (13) is because of the optimization variables that are complex numbers and the operators that calculate the absolute values. All these sources of non-linearity can be removed by adding the new variables $G^{h,re}_{(i,j)}$, $G^{h,im}_{(i,j)}$, $G^{re}_{(i,j)}$, and $G^{im}_{(i,j)}$ and the following new constraints to the optimization problem (13):

$$-G^{h,re}_{(i,j)} \le \frac{\mathrm{Re}\{I^{h}_{(i,j)} - I^{h,m}_{(i,j)}\}}{|\mathrm{Re}\{I^{h,m}_{(i,j)}\}|} \le G^{h,re}_{(i,j)} \ \forall (i,j) \in \mathcal{M} \tag{23}$$

$$-G^{h,im}_{(i,j)} \le \frac{\mathrm{Im}\{I^{h}_{(i,j)} - I^{h,m}_{(i,j)}\}}{|\mathrm{Im}\{I^{h,m}_{(i,j)}\}|} \le G^{h,im}_{(i,j)} \ \forall (i,j) \in \mathcal{M} \tag{24}$$

$$-G^{re}_{(i,j)} \le \frac{\mathrm{Re}\{I_{(i,j)} - I^{m}_{(i,j)}\}}{|\mathrm{Re}\{I^{m}_{(i,j)}\}|} \le G^{re}_{(i,j)} \ \forall (i,j) \in \mathcal{M} \tag{25}$$

$$-G^{im}_{(i,j)} \le \frac{\mathrm{Im}\{I_{(i,j)} - I^{m}_{(i,j)}\}}{|\mathrm{Im}\{I^{m}_{(i,j)}\}|} \le G^{im}_{(i,j)} \ \forall (i,j) \in \mathcal{M}. \tag{26}$$

As a result, the problem in (13) can be reformulated to the following MILP:

$$\begin{aligned} \textbf{Min} \quad & \sum_{(i,j)\in\mathcal{M}} G^{h,re}_{(i,j)} + G^{h,im}_{(i,j)} + G^{re}_{(i,j)} + G^{im}_{(i,j)} \\ \textbf{s.t.} \quad & \text{Eqs } (2) \sim (3), (8) \sim (12), (14) \sim (26). \end{aligned} \tag{27}$$

Please note that because there are no approximations in the process of reformulating the MINLP problem to the MILP problem, the replaced constraints and modified objective functions in MILP are equivalent to the ones in MINLP; hence the MINLP problem (13) is equal to the MILP problem (27).

V. Observability Analysis and Discussion on the Harmonic Sources

A. Observability of the SSI Scheme only Using Harmonic Currents

Here, we provide an analysis on the number of and location of harmonic sources and PMUs that are needed to ensure full observability of the DN. For simplifying the analysis we consider an SSI scheme that utilizes only harmonic current measurements:

$$\begin{aligned} \textbf{Min} \quad & \sum_{(i,j)\in\mathcal{M}} G^{h,re}_{(i,j)} + G^{h,im}_{(i,j)} \\ \textbf{s.t.} \quad & \text{Eqs } (2)\sim(3), (10)\sim(12), (14)\sim(26). \end{aligned} \tag{28}$$

We define an *independent* loop as a loop that doesn't include any other loop within. We have the following theorem:

Theorem 1: *Consider a DN in which a PMU is placed in each independent loop. The status of all switches in this DN could be identified using only the harmonic current measurements, if there is a harmonic source at each node of the DN.*

Proof:

- Step 1: we show that under the said condition, all harmonic current paths can be detected. For a loop with N_l nodes, there are also N_l branches. One can formulate N_l equations on the currents flowing in the N_l branches of the loop based on (2), where each equation corresponds to a known harmonic injection that is equal to a harmonic source current. However, only $N_l - 1$ equations are independent [17]. Another independent equation can be formulated for the measurement performed by the PMU that is placed in the loop. For example, if a PMU is placed at branch $(n, n+1)$ of the loop in Fig. 1, then an independent equation $I^h_{(n,n+1)} = I^{h,m}_{(n,n+1)}$ is considered for the measurement of this PMU. In overall, the N_l formulated equations will provide a *unique* solution to the currents flowing in N_l branches of the loop. This solution is then used along with (7) to calculate numerical values of the binary variables $b^h_{(i,j)}$. Consequently, all harmonic current paths in the DN can be detected.
- Step 2: A branch that falls on a harmonic current path can be identified as closed. To complete the proof of the theorem, we only need to show that a branch must be open if it doesn't fall on any harmonic current path. To this end, let $(n, n+1)$ denote a branch carrying no harmonic current. There must be two different harmonic current paths from node n to the substation and from node $n+1$ to the substation, to carry the harmonic currents generated by the harmonic sources at nodes n and $n+1$. The two harmonic current paths don't include the branch $(n, n+1)$ since it is assumed that no harmonic current flows through it. The branches on the said two harmonic currents paths together with the branch $(n, n+1)$ make a loop, in which the branch $(n, n+1)$ is the only one with no harmonic current. Therefore, from Section II the branch $(n, n+1)$ must be open to preserve the radial topology of the DN.

B. PMU Placement for Full Observability of the Proposed SSI Scheme

Base on the above analysis, if there is a PMU placed in each independent loop of the DN, the SSI problem that uses only harmonic measurements comes with a solution for the harmonic current flowing through each branch. This is still true even though only a few nodes may have harmonic sources, because the harmonic current injections of the nodes with no harmonic sources are almost 0. Similarly, the SSI problem that uses fundamental measurements comes with a solution for the fundamental current flowing through each branch, if there is a PMU placed in each independent loop of the DN, as the fundamental current injection of each node would be known. When the fundamental and harmonic currents flowing through each branch are obtained, all switch status for the DN can be identified. Thus, we can conclude that when there is at least one PMU placed in each independent loop, the proposed SSI scheme will have a full observability.

C. Observability of the Proposed SSI Scheme in the Presence of DGs

Due to the usage of inverters, DGs may also be sources of harmonic currents. Power quality sensors are generally used to monitor harmonic currents generated by large DGs. However, the harmonic currents generated by small DGs may not be monitorable as they may not be equipped with monitoring devices. This paper assumes that the harmonic currents generated by the small DGs are 0 because the currents of these harmonic sources are generally very small; see [27].

The DGs can also cause reverse power flow on the fundamental side. This issue is handled by the SSI scheme on the fundamental side; see (8) and (9). More specifically, a generation output will be considered in (8) when there is a DG which can cause reverse power flow.

D. Discussion on the Types of Harmonic Sources

In DNs, nonlinear industrial and commercial loads, e.g., motors and power electronic devices used in various industrial pumps, arc furnace, rolling mill and large DG stations can introduce a significant number of large harmonic sources [28]. Generally, there are power quality sensors to monitor these large harmonic sources. However, there are some nonlinear residential loads in the DN, which only introduce few harmonic currents. Also, no power quality sensors are equipped with these loads. Thus, the proposed SSI scheme is useful in the SSI problem where the DNs have nonlinear industrial and commercial loads. If the DN loads are all residential loads and there are no large harmonic sources, the proposed SSI scheme can't be applied.

VI. Performance Evaluation: IEEE 33-Bus Power System

In this section, IEEE 33-bus power system [29] is used for assessing the performance of the proposed SSI scheme. Unless stated otherwise, six harmonic sources are randomly located at the 33-bus system, and the magnitudes of the

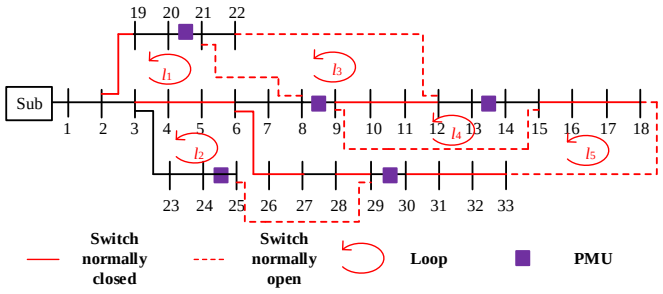

Fig. 3. The IEEE 33-bus power system includes five independent loops, where in each independent loop a PMU is placed. The red dotted and red dashed lines are normally open and closed lines, respectively. The black lines are just distribution lines without switches. Six harmonic sources are randomly located at the 33 buses.

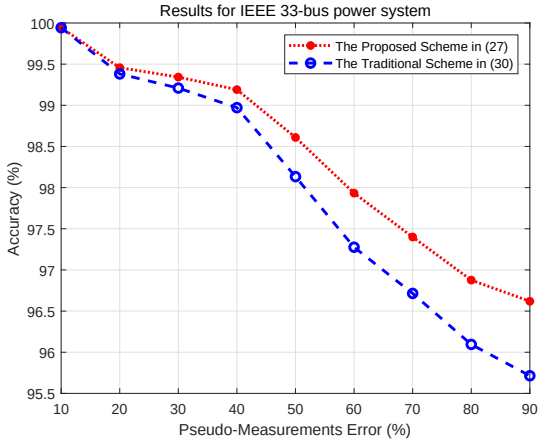

Fig. 4. The accuracy of the proposed and the traditional SSI schemes against errors in pseudo-measurements. Fundamental branch current, harmonic branch current and harmonic source measurement errors are all set to 0.

harmonic source currents are set referred to [30], where there is data particularly on the 3rd harmonic current of phase A. This choice of data is following the fact that, the 3rd harmonic currents come with the largest magnitudes. There are 5 independent loops in the feeder under study as shown in Fig. 3. In each independent loop a PMU is placed, and thus the SSI problem is solvable. Synthesized measurements of branch harmonic currents and harmonic sources are obtained from MATLAB, where the load is modeled based on the Model A given in [22]. The measurements are contaminated according to the Gaussian distribution, where the standard deviation is calculated based on the percentage of the original values; see [31]. We assume there are 21 switches in the 33-bus system, and 20 radial topologies involving modifications with respect to each independent loop are selected for the numerical simulations. Unless stated otherwise, the threshold parameter c is set to 25% of the parameter z. The results are obtained based on Monte Carlo simulation with 1000 iterations for each test case. The accuracy of the SSI schemes can be obtained according to the following formula:

$$\text{Accuracy} = \frac{N_{\text{correct}}}{N_{\text{total}}} \times 100\%, \tag{29}$$

where N_{total} is the total number of switches in all the tests and N_{correct} is the number of the switches with a correct output being produced. For an SSI scheme that utilizes only the measurements of harmonic currents, i.e., the problem (28), the correct output refers to the correct identification of the status of the switches on the harmonic current paths. For the proposed scheme in (27) and the traditional SSI scheme, the correct output refers to the correct status of the switches of the DN. The switch status of the DN resulted from the traditional SSI scheme is obtained by solving the following optimization problem:

$$\begin{aligned} \textbf{Min} \quad & \sum_{(i,j)\in\mathcal{M}} G^{re}_{(i,j)} + G^{im}_{(i,j)} \\ \textbf{s.t.} \quad & \text{Eqs } (8) \sim (9), (11) \sim (12). \end{aligned} \tag{30}$$

A. The Overall Performances of the Proposed Scheme

As discussed in section I, the main source of error in the traditional SSI scheme is the errors in pseudo-measurements. The pseudo-measurements of fundamental current injections are estimated using the historical load curves and the nodal voltages [20]. The load curves can be obtained from the smart meters [32]–[34]. The reporting intervals of the smart meters and the PMUs could be different. Under this condition, the SSI will be performed with a longer time interval to be in line with the lower-resolution data. For an industrial system, the load curve could have few changes, and the pseudo-measurement error will be small. However, for a residential grid, it is difficult to obtain an accurate load curve for every bus. In order to simulate the worst conditions, the largest pseudo-measurement error is considered as 90%.

The results show that for the case of various pseudo-measurement errors, the SSI only using harmonic current information can correctly detect all the branches on harmonic current paths. Further, Fig. 4 shows the accuracy of the proposed and the traditional SSI schemes for a various percentage of errors in the pseudo-measurements. From Fig. 4, we can see that even in different scenarios with different pseudo-measurement errors, the accuracy of the proposed SSI scheme is always higher than 90%, which shows the proposed SSI scheme can actually solve the real SSI problem in DNs. Also, the accuracy of the proposed scheme is always higher than that of the traditional scheme. As the percentage of error in pseudo-measurement increases, the accuracy of both schemes decreases. When the percentage of error in pseudo-measurement becomes 90%, the proposed SSI scheme can correct over 20% wrong identification results returned by the traditional SSI scheme.

Fig. 4 also shows that, for 10% error in pseudo-measurements, the accuracy of the proposed and the traditional SSI schemes are almost the same. This result is justifiable by the fact that, the incorrect estimated status in the traditional SSI scheme correspond to switches that are not on any harmonic current path and consequently cannot be corrected by the proposed SSI scheme. The better performance of the proposed SSI scheme compared to the traditional scheme is seen especially when the percentage of error in pseudo-

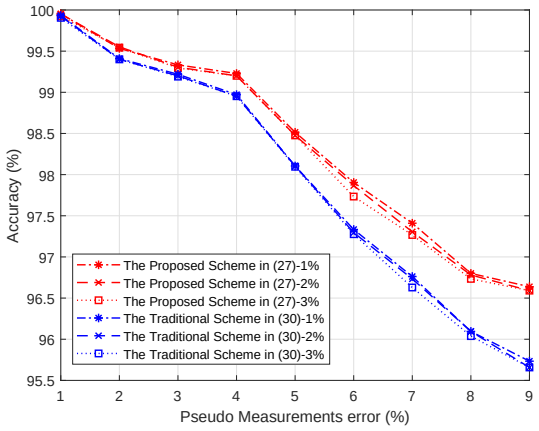

Fig. 5. The accuracy of the proposed and the traditional SSI schemes with joint fundamental measurement errors. Harmonic branch current and harmonic source measurement errors are both set to 0.

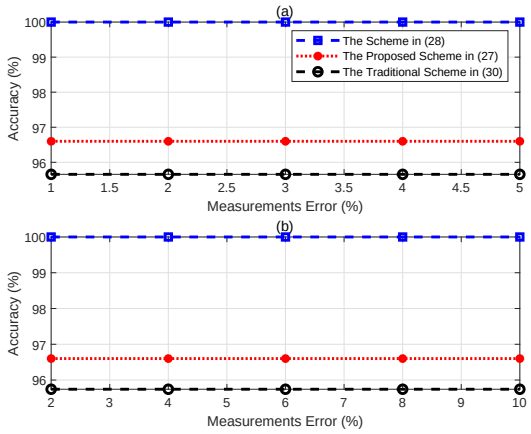

Fig. 6. The accuracy of the SSI schemes under (a) erroneous harmonic current measurements and (b) erroneous harmonic source measurements. The fundamental branch current and pseudo fundamental injection measurement errors are 3% and 90%, respectively.

measurements becomes more than 10%.

It should be noted that the locations of the harmonic sources could have an impact on the SSI accuracy. First of all, the location of harmonic sources impacts the harmonic current paths. If the switches whose status are incorrectly identified by the SSI scheme which merely uses fundamental information are not on a harmonic current path, then the incorrectly identified status of such switches cannot be corrected by the SSI scheme that uses harmonic information. Second, when the harmonic sources are located close to the substation, the impact of the harmonic measurements on the SSI accuracy is marginal because just a small portion of distribution lines are placed on the harmonic paths. As a result, few switch status can be corrected by the proposed SSI scheme.

It should also be noted that the proposed SSI scheme and the traditional SSI scheme both have accuracy over 90%. This is because almost only the status of the switches close to the end of the laterals and also far away from the PMUs has the chance to be wrongly identified by the both SSI schemes. For example, for the topology shown in Fig. 3, almost only the status of the switches (32, 33), (17, 18), and (18, 33) has the chance to be wrongly identified. If the status of other switches is wrongly identified, there will be large differences between the fundamental branch current measurements and the corresponding estimates returned by the both SSI schemes. As a result, such wrong identification events rarely happen in reality. Although this paper only consider 20 topologies, the proposed SSI scheme will still have high accuracy for the identification of other valid topologies.

B. The Impact of Erroneous Fundamental Current Measurements

We repeat the same numerical case study discussed in Section VI-A with a minor change in the simulation setup, by considering erroneous fundamental branch current measurements. The range of total vector error (TVE) in the PMU fundamental current measurement is set to 1% to 3%, following the IEEE Std. C37.118.1-2011 [35]. The corresponding results are shown in Fig. 5. For various percentage of pseudo-measurements, the accuracy of the proposed and the traditional SSI schemes are almost identical to the case with errorless PMUs data. This again shows the outperformance of the proposed SSI scheme compared to the traditional SSI scheme for the case of erroneous PMU measurements.

C. The Impact of Erroneous Harmonic Branch Current Measurements and Harmonic Source Measurements

This section assesses the impact of erroneous harmonic branch current measurements and harmonic source measurements on the accuracy of the SSI schemes. First, we study the impact of erroneous harmonic branch current measurements. We consider a scenario where there are 1% to 5% TVE in the PMU harmonic current measurement, 90% error in the pseudo-measurements, and 3% error in the measurements of fundamental currents flowing through the branches. From Fig. 6(a), for the case of erroneous harmonic current measurements all the branches on harmonic current paths can still be detected correctly. Also, the proposed SSI scheme can still correct over 20% wrong identification results returned by the traditional SSI scheme. Therefore, it can be observed that the proposed SSI scheme is robust to the errors in harmonic currents measurements.

To justify this observation, first, we notice that the value of the threshold is less than the value of the contaminated harmonic current measurement. As a result, the harmonic current paths can be identified correctly. Second, the problem (27) minimizes the total error in the estimation of harmonic and fundamental currents. Since the harmonic currents are scattered all around the power system, incorrect identification of a branch that actually falls on a harmonic current path is much more impactful on the objective function of problem (27), compared to incorrect identification of a switch status in the traditional SSI scheme that uses fundamental current measurements. For instance, the incorrect identification of the harmonic current path generated by a current source may

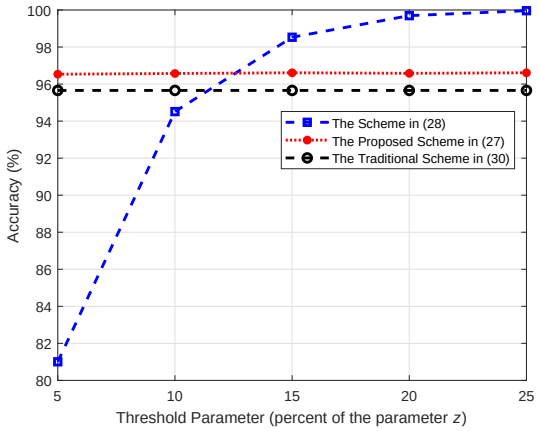

Fig. 7. The impact of threshold parameter on SSI accuracy (%).The errors in harmonic currents, harmonic sources, pseudo-measurements, and fundamental currents are 5%, 10%, 90% and 3%, respectively.

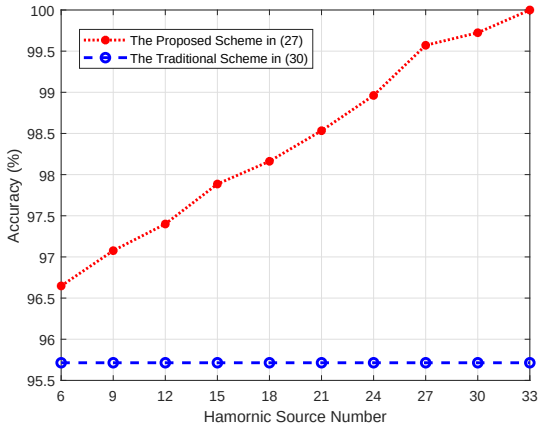

Fig. 8. The impact of the number of harmonic source on SSI accuracy (%). The pseudo fundamental injection measurement errors is 90%. Fundamental branch current, harmonic branch current and harmonic source measurement errors are all set to 0.

increase the objective function of problem (27) by more than 1. In contrast, incorrect identification of a switch status may increase the same objective function by only a few hundredth of 1. In conclusion, the optimization problem (27) tends to be robust to the errors in harmonic current measurements.

The measurements of harmonic sources are performed by the power quality devices that are located at the loads. They may produce a level of error larger than the error being produced by PMUs. Accordingly, in this section, we consider harmonic source measurements with up to 10% error. The values of errors set in pseudo-measurements and fundamental current measurements are 90% and 3%, respectively. Fig. 6(b) shows the accuracy of the SSI schemes for a various percentage of harmonic source TVE. From Fig. 6(b), the proposed SSI scheme is robust to the errors in harmonic source measurements. This observation is justifiable by a reasoning similar to the one mentioned earlier.

D. The Impact of the Threshold Parameter

The threshold parameter c should be set in a way that, in the proposed SSI scheme the impact of errors in harmonic sources and harmonic currents are lowered. In this section, the threshold parameter is set to various levels from 5 to 25 percent of the parameter z defined in section III-A. The errors in harmonic currents, harmonic sources, pseudo-measurements, and fundamental currents are 5%, 10%, 90% and 3%, respectively.

Fig. 7 shows the accuracy of the SSI schemes for various values of the threshold parameter c. A low value for the threshold parameter, e.g. $c = 5\%z$ may lead to incorrect detection of some branches actually not on a harmonic current path. For the SSI scheme that uses only harmonic current measurements, this can result in incorrect identification of some branch status, as it can be seen from the blue dotted line in Fig. 7. In contrast, the accuracy of the proposed SSI scheme is the same for various values of the threshold parameter c. This is due to the fact that, the proposed SSI scheme in (27) utilizes the fundamental current measurements to identify the switch status correctly, even if some branch status are identified incorrectly. Consequently, we can observe that the proposed SSI scheme is robust to the choice of the threshold parameter c because of using both the harmonic and fundamental measurements together.

E. The Impact of the Number of Harmonic Sources

In this section, we study the impacts of the number of harmonic sources on SSI accuracy. Here, we still assume that five PMUs are installed in our test system as shown in Fig. 3. It is assumed that when there are n harmonic sources in the test network, then these harmonic sources are randomly located at the 33-bus system. It is assumed that there are no harmonic measurement errors, and the threshold parameter c is set to 10% of the parameter z. The errors in pseudo-measurements are set to 90%.

The accuracy of the SSI schemes for different number of harmonic sources are shown in Fig. 8. As the number of harmonic sources increases, the accuracy of the proposed SSI scheme increases. This is because by having more harmonic sources, more switches fall on harmonic current paths, which help the proposed SSI scheme to correctly derive the status of the switches that would be identified incorrectly if one uses only the fundamental current measurements. Also, the proposed SSI scheme works with 100% accuracy when the number of harmonic sources is equal to the number of nodes in the DN, which is explained as a requirement for full observability in theorem 1.

There is a chance that the proposed SSI scheme works with 100% accuracy even with fewer sources. For instance, when there are harmonic sources located at the end of all the laterals, all the closed switches fall on at least one harmonic current path, and the proposed SSI scheme also achieves 100% accuracy. However, in an SSI problem, the real topology of the DN, i.e., the end of the lateral is unknown. As a result, this conclusion can't be used for enhancing SSI accuracy. The theorem 1 gives a sufficient condition to make sure that all closed switches fall on at least one harmonic current path, which consequently leads to 100% accuracy.

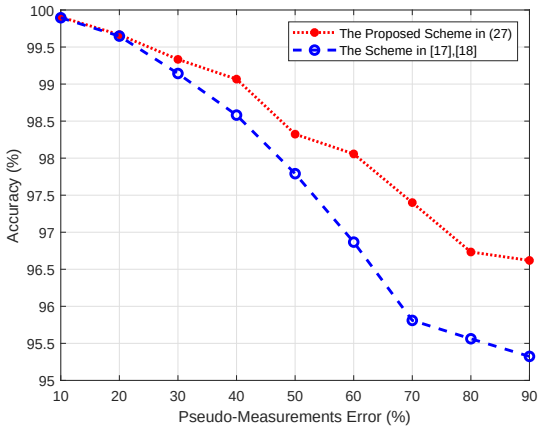

Fig. 9. The accuracy of the proposed SSI scheme and the SSI scheme modified from [17], [18] under different pseudo-measurement errors. The fundamental branch current measurement error is 3%. Harmonic branch current and harmonic source measurement errors are both set to 0.

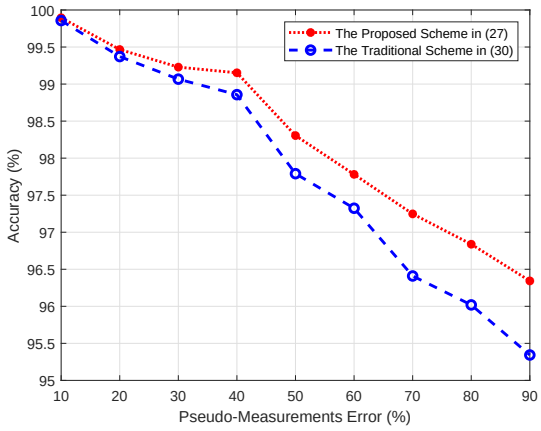

Fig. 10. Accuracy of the proposed and traditional SSI schemes when there exist small DGs.The fundamental branch current and pseudo fundamental injection measurement errors are 3% and 90%, respectively. Harmonic branch current and harmonic source measurement errors are both set to 0.

F. Performance Comparisons with Other Existing SSI Schemes

This section compares the performances of the proposed SSI scheme with other existing SSI schemes developed in recently published references [17], [18], which are MILP-based SSI schemes that use only fundamental measurements. To make different schemes comparable, the proposed SSI method in [17], [18] are modified to add constraints (11)-(12) to ensure radial topologies. Also, fundamental branch current and fundamental injection errors instead of power injection errors are set as the variables of the objective function [17]. The TVE of fundamental branch currents is set to 3%. The level of error in the fundamental pseudo-current injections are set from 10% to 90% in incremental steps of 10%. The results are shown in Fig. 9. As it can be seen, the proposed SSI scheme is still more accurate than the SSI scheme inspired from [17], [18]. When the error in pseudo-current injections is 90%, the proposed SSI scheme can still correct over 20% wrong identification results returned by the traditional SSI scheme.

G. The Impact of Small DGs

As discussed in section V-C, the harmonic source currents of small DGs are assumed as 0 due to their relatively small magnitudes compared with large harmonic sources [27]. In this section, numerical simulations are included to examine the performance of the proposed SSI scheme in the presence of small DGs. We assume that there are 5 small DGs which is randomly located at the 33-bus network. As the DGs usually lead to higher uncertainties in power consumptions, the pseudo-current injection errors of the corresponding nodes are set to be 5% higher than other pseudo-current injections. In order to simulate the worst case scenario, we assume that the harmonic current of each harmonic source generated from each small DG is 10% of the largest harmonic source current in the original simulation setup that excluded DGs. The corresponding results are shown in Fig. 10.

As seen from Fig. 10, the advantage of the proposed SSI scheme over the traditional SSI scheme is still considerable, even when there are small DGs with unknown harmonic source currents. Also, when there is 90% error in pseudo-measurements, the proposed SSI scheme can still correct over 20% wrong identification results returned by the traditional SSI scheme. This observation indicates that operation of small DGs with non-zero harmonic currents in the DN doesn't reduce the advantage of the proposed SSI scheme. By comparing Fig. 10 and Fig. 4, we can see that the DGs lead to lower accuracy on the both SSI schemes.

VII. Performance Evaluation: IEEE 123-Bus Power System

In this section, we evaluate the performance of the SSI scheme on the IEEE 123-bus power system [36] which resembles a large real-life DN, and shown in Fig. 11. The simulations are carried out in MATLAB R2015a by using the *intlinprog* solver on a laptop with 8 GB RAM and 2.3 GHz CPU. Ten harmonic sources are located at the nodes with loads randomly; with current phasors $1\angle 0°$ A. To test the proposed scheme in a complicated configuration, the IEEE 123-bus system is modified to have 10 independent loops. Accordingly, there is a PMU placed in each independent loop. Considering that the three-phase 123 bus system is an unbalanced system, the positive fundamental currents and harmonic currents are used for SSI. To justify the usefulness of such a simplification, we note that the switch status of the three phases are changed simultaneously. If the switch status is detected by using the positive sequence information, the switch status of negative and zero sequences are also automatically detected. As a result, the status of the three phase switches are all detected. The simulation results validate the usefulness of such a simplification.

The error in pseudo-current injection is set to various levels from 10% to 90% in incremental steps of 10%. The results are shown in Fig. 12. As it can be seen, even though there is 90% error in pseudo-measurements, the accuracy of the proposed and the traditional SSI schemes are still higher than 90%. These results validate that the simplification of using

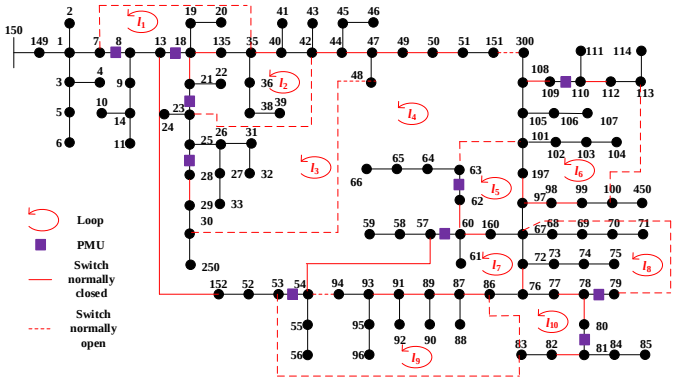

Fig. 11. The IEEE 123-bus power system includes ten independent loops, where in each independent loop a PMU is placed. The red dotted and red dashed lines are normally open and closed lines, respectively. Other lines are just distribution lines without switches. Ten harmonic sources are randomly located at the buses with loads.

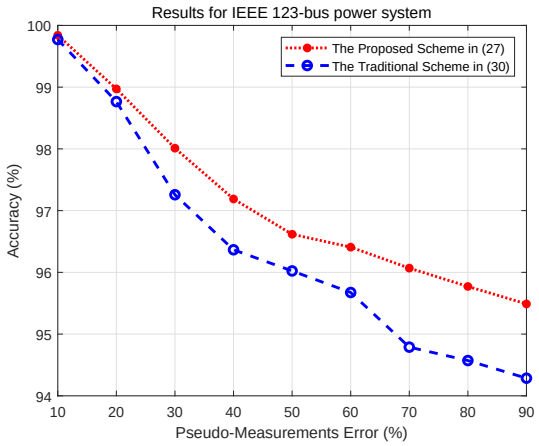

Fig. 12. The accuracy of the proposed SSI scheme and the traditional SSI scheme in the test case of IEEE 123-bus power system. Fundamental branch current, harmonic branch current and harmonic source measurement errors are all set to 0.

positive sequence information for SSI is useful. By comparing the proposed and the traditional schemes, we can see that as the error in pseudo-measurements increases, the proposed SSI scheme becomes more and more accurate than the traditional SSI scheme. When the error in pseudo-measurements is 90%, the proposed SSI scheme can correct about 20% wrong results returned by the traditional SSI scheme. This is because the harmonic measurements integrated in the proposed SSI scheme becomes effective in correcting the status of the switches that are identified incorrectly by using only fundamental measurements. The average computation time is about 120 s. Please note the main computation time is for the SSI under large pseudo-measurement error condition. If 20% or less error is considered, the average computation time is less than 35 s.

VIII. Conclusion

In this paper, a novel switch status identification (SSI) scheme was proposed for radial distribution networks (DNs). The proposed SSI scheme uses both the harmonic and fundamental current measurements to enhance the SSI accuracy in DNs. Through numerical simulations on IEEE 33-Bus power system, it was shown that the proposed SSI scheme can correct over 20% wrong results returned by the traditional SSI scheme that uses only measurements of fundamental currents. Also, it was shown that the proposed SSI scheme is robust to the errors in harmonic and fundamental current measurements. Even though there are small DGs in the DNs and no harmonic monitoring devices are installed to measure their harmonic currents, the proposed SSI scheme is still more accurate than the traditional SSI scheme. Furthermore, a theoretical analysis was provided on the observability of the DN using harmonic current measurements. Accordingly, a case study is shown that the proposed SSI scheme will work with 100% accuracy when the number of harmonic sources is equal to the number of nodes in the DN. The simulation results in IEEE 123-bus power system confirm the advantage over the traditional SSI scheme. Future works include: 1) proposing an SSI scheme for meshed distribution systems using harmonic current measurements; 2) proposing an SSI scheme by using multiple harmonic components to improve the SSI redundancy.

References

[1] M. Farajollahi, A. Shahsavari, E. M. Stewart, and H. Mohsenian-Rad, "Locating the source of events in power distribution systems using micro-PMU data," *IEEE Trans. Power Syst.*, vol. 33, no. 6, pp. 6343–6354, Nov 2018.

[2] A. Primadianto and C. Lu, "A review on distribution system state estimation," *IEEE Trans. Power Syst.*, vol. 32, no. 5, pp. 3875–3883, Sep 2017.

[3] P. A. Pegoraro, K. Brady, P. Castello, C. Muscas, and A. von Meier, "Line impedance estimation based on synchrophasor measurements for power distribution systems," *IEEE Trans. Instrum. Meas.*, vol. 68, no. 4, pp. 1002–1013, Apr 2019.

[4] A. Carta, N. Locci, and C. Muscas, "GPS-based system for the measurement of synchronized harmonic phasors," *IEEE Trans. Instrum. Meas.*, vol. 58, no. 3, pp. 586–593, Mar 2009.

[5] ——, "A PMU for the measurement of synchronized harmonic phasors in three-phase distribution networks," *IEEE Trans. Instrum. Meas.*, vol. 58, no. 10, pp. 3723–3730, Oct 2009.

[6] L. Chen, W. Zhao, Q. Wang, F. Wang, and S. Huang, "Dynamic harmonic synchrophasor estimator based on sinc interpolation functions," *IEEE Trans. Instrum. Meas.*, vol. 68, no. 9, pp. 3054–3065, Sept 2019.

[7] L. Chen, W. Zhao, F. Wang, and S. Huang, "Harmonic phasor estimator for p class phasor measurement units," *IEEE Trans. Instrum. Meas.*, vol. 69, no. 4, pp. 1556–1565, May 2020.

[8] N. Kanao, M. Yamashita, H. Yanagida, M. Mizukami, Y. Hayashi, and J. Matsuki, "Power system harmonic analysis using state-estimation method for japanese field data," *IEEE Trans. Power Del.*, vol. 20, no. 2, pp. 970–977, Apr 2005.

[9] Y. Weng, Y. Liao, and R. Rajagopal, "Distributed energy resources topology identification via graphical modeling," *IEEE Trans. Power Syst.*, vol. 32, no. 4, pp. 2682–2694, Jul 2017.

[10] S. Bolognani, N. Bof, D. Michelotti, R. Muraro, and L. Schenato, "Identification of power distribution network topology via voltage correlation analysis," in *Proc. of 52nd IEEE Conf. on Decision and Control*, Florence, Italy, 2013, pp. 1659–1664.

[11] G. Cavraro and V. Kekatos, "Graph algorithms for topology identification using power grid probing," *IEEE Control Systems Letters*, vol. 2, no. 4, pp. 689–694, Oct 2018.

[12] J. Yu, Y. Weng, and R. Rajagopal, "Patopa: A data-driven parameter and topology joint estimation framework in distribution grids," *IEEE Trans. Power Syst.*, vol. 33, no. 4, pp. 4335–4347, Jul 2018.

[13] O. Ardakanian, V. W. S. Wong, R. Dobbe, S. H. Low, A. von Meier, C. J. Tomlin, and Y. Yuan, "On identification of distribution grids," *IEEE Trans. Control of Network Syst.*, vol. 6, no. 3, pp. 950–960, Sept 2019.

[14] J. Zhang, Y. Wang, Y. Weng, and N. Zhang, "Topology identification and line parameter estimation for non-pmu distribution network: A numerical method," *IEEE Trans. Smart Grid*, pp. 1–1, Mar 2020.

[15] J. Yu, Y. Weng, and R. Rajagopal, "Patopaem: A data-driven parameter and topology joint estimation framework for time-varying system in distribution grids," *IEEE Trans. Power Syst.*, vol. 34, no. 3, pp. 1682–1692, May 2019.

[16] G. Cavraro and R. Arghandeh, "Power distribution network topology detection with time-series signature verification method," *IEEE Trans. Power Syst.*, vol. 33, no. 4, pp. 3500–3509, Jul 2018.

[17] M. Farajollahi, A. Shahsavari, and H. Mohsenian-Rad, "Topology identification in distribution systems using line current sensors: An milp approach," *IEEE Trans. Smart Grid*, vol. 11, no. 2, pp. 1159–1170, Mar 2020.

[18] A. Gandluru, S. Poudel, and A. Dubey, "Joint estimation of operational topology and outages for unbalanced power distribution systems," *IEEE Trans. Power Syst.*, vol. 35, no. 1, pp. 605–617, Jan 2020.

[19] Z. Tian, W. Wu, and B. Zhang, "A mixed integer quadratic programming model for topology identification in distribution network," *IEEE Trans. Power Syst.*, vol. 31, no. 1, pp. 823–824, Jan 2016.

[20] A. Abur, D. Shirmohammadi, and C. S. Cheng, "Estimation of switch statuses for radial power distribution systems," in *Proc. of IEEE Int. Symp. Circuits and Syst.*, vol. 2, Seattle, WA, USA, 1995.

[21] D. Montenegro, R. Dugan, and G. Ramos, "Harmonics analysis using sequential-time simulation for addressing smart grid challenges," in *Proc. of 23rd Int. Conf. Electricity Distribution*, Lyon, France, 2015.

[22] T. F. on Harmonics Modeling and Simulation, "Modeling and simulation of the propagation of harmonics in electric power networks. i. concepts, models, and simulation techniques," *IEEE Trans. Power Del.*, vol. 11, no. 1, pp. 452–465, Jan 1996.

[23] H. Fujita, T. Yamasaki, and H. Akagi, "A hybrid active filter for damping of harmonic resonance in industrial power systems," *IEEE Trans. Power Electron.*, vol. 15, no. 2, pp. 215–222, Mar 2000.

[24] Harmonic measurement in electrical networks, schneider electric, 2020. [Online]. Available: https://www.electrical-installation.org/enwiki/Harmonic_measurement_in_electrical_networks/

[25] D. Andrews, M. T. Bishop, and J. F. Witte, "Harmonic measurements, analysis, and power factor correction in a modern steel manufacturing facility," *IEEE Trans. Ind. Appl.*, vol. 32, no. 3, pp. 617–624, May/Jun 1996.

[26] H. N. Gabow and E. W. Myers, "Finding all spanning trees of directed and undirected graphs," *Siam Journal on Computing*, vol. 7, no. 3, pp. 280–287, Aug 1978.

[27] Y. D. Lee, C. S. Chen, C. T. Hsu, and H. S. Cheng, "Harmonic analysis for the distribution system with dispersed generation systems," in *Proc. of 2006 Int. Conf. on Power Syst. Technology*, Chongqing, China, 2006, pp. 1–6.

[28] D. Kumar and F. Zare, "Harmonic analysis of grid connected power electronic systems in low voltage distribution networks," *IEEE Journal of Emerging and Selected Topics in Power Electronics*, vol. 4, no. 1, pp. 70–79, 2016.

[29] M. E. Baran and F. F. Wu, "Network reconfiguration in distribution systems for loss reduction and load balancing," *IEEE Trans. Power Del.*, vol. 4, no. 2, pp. 1401–1407, Apr 1989.

[30] I. D. Melo, J. L. Pereira, A. M. Variz, and P. A. Garcia, "Harmonic state estimation for distribution networks using phasor measurement units," *Electr. Power Syst. Res.*, vol. 147, pp. 133–144, Jun 2017.

[31] R. Singh, B. C. Pal, and R. B. Vinter, "Measurement placement in distribution system state estimation," *IEEE Trans. Power Syst.*, vol. 24, no. 2, pp. 668–675, May 2009.

[32] Y. R. Gahrooei, A. Khodabakhshian, and R. Hooshmand, "A new pseudo load profile determination approach in low voltage distribution networks," *IEEE Trans. Power Syst.*, vol. 33, no. 1, pp. 463–472, 2018.

[33] A. Al-Wakeel, J. Wu, and N. Jenkins, "k-means based load estimation of domestic smart meter measurements," *Applied Energy*, vol. 194, pp. 333 – 342, 2017.

[34] D. T. Nguyen, "Modeling load uncertainty in distribution network monitoring," *IEEE Trans. Power Systems*, vol. 30, no. 5, pp. 2321–2328, 2015.

[35] *IEEE Standard for Synchrophasor Measurements for Power Systems*. IEEE Std C37.118.1-2011 (Revision of IEEE Std C37.118-2005), Dec 2011.

[36] Radial distribution test feeders, distribution system analysis subcommittee rep., 2020. [Online]. Available: https://site.ieee.org/pes-testfeeders/resources/

Lei Chen (S′ 19) received the B.Sc. degree from North China Electric Power University, Baoding, China, in 2015, and the PhD degree from Tsinghua University, Beijing, China, in 2020. He was a visiting PhD student with the University of California, Riverside, CA, US, in 2019. He is currently a postdoctoral fellow with the Department of Electrical Engineering, Tsinghua University.

His current research interests include power system wide area monitoring, phasor measurement unit algorithms, new synchrophasor applications, and power system wideband oscillation analysis and control.

Mohammad Farajollahi (S′ 15) received the B.Sc. degree in Electrical Engineering from University of Tehran, Tehran, Iran, in 2014, the M.Sc. degree in electrical engineering from Sharif University of Technology, Tehran, in 2016, and the Ph.D. degree at University of California, Riverside, CA, US, in 2020. His research interests include power system planning, operation, reliability, as well as optimization. He is specifically working on applications of micro-PMUs and data analysis in distribution system monitoring.

Mahdi Ghamkhari is an assistant professor at the Electrical and Computer Engineering Department of University of Louisiana at Lafayette. Before becoming a faculty, he was a postdoctoral scholar at University of California, Berkeley. Prior to that, he was a postdoctoral scholar at University of California, Davis. He received his Ph.D. degree from University of California, Riverside, his Master of Science degree from Texas Tech University, and his Bachelor of Science degree from Sharif University of Technology. His research focuses on optimization of energy systems.

Wei Zhao received the Ph.D. degree from the Moscow Energy Institute, Moscow, Russia, in 1991. He is currently a Professor with the Department of Electrical Engineering, Tsinghua University, Beijing, China.

His current research interests include electromagnetic measurement, virtual instrumentation, networked instrumentation system, and cloud-based instrumentation.

Songling Huang (SM′ 18) received the Ph.D. degree from Tsinghua University, Beijing, China, in 2001. He is currently a Professor with the Department of Electrical Engineering, Tsinghua University.

His current research interests include electromagnetic measurement and nondestructive evaluation.

Hamed Mohsenian-Rad (F'20) received the Ph.D. degree in electrical and computer engineering from the University of British Columbia, Vancouver, BC, Canada, in 2008. He is currently a Professor of electrical engineering and Bourns Family Faculty Fellow at the University of California, Riverside, CA, USA. His research interests include monitoring, data analysis, and optimization of power systems and smart grids. He is the author of the book *Smart Grid Sensors: Principles and Applications*. He was the recipient of the National Science Foundation CAREER Award, the Best Paper Award from the IEEE Power and Energy Society General Meeting, and the Best Paper Award from the IEEE Conference on Smart Grid Communications. He is an Editor of the IEEE TRANSACTIONS ON SMART GRID and the IEEE POWER ENGINEERING LETTERS.